

A Linear AC-OPF Formulation for Unbalanced Distribution Networks

Giraldo, Juan S.; Vergara Barrios, P.P.; Lopez, Juan Camilo; Nguyen, Phuong H. ; Paterakis, Nikolaos G.

DOI

[10.1109/TIA.2021.3085799](https://doi.org/10.1109/TIA.2021.3085799)

Publication date

2021

Document Version

Accepted author manuscript

Published in

IEEE Transactions on Industry Applications

Citation (APA)

Giraldo, J. S., Vergara Barrios, P. P., Lopez, J. C., Nguyen, P. H., & Paterakis, N. G. (2021). A Linear AC-OPF Formulation for Unbalanced Distribution Networks. *IEEE Transactions on Industry Applications*, 57(5), 4462-4472. Article 9444771. <https://doi.org/10.1109/TIA.2021.3085799>

Important note

To cite this publication, please use the final published version (if applicable). Please check the document version above.

Copyright

Other than for strictly personal use, it is not permitted to download, forward or distribute the text or part of it, without the consent of the author(s) and/or copyright holder(s), unless the work is under an open content license such as Creative Commons.

Takedown policy

Please contact us and provide details if you believe this document breaches copyrights. We will remove access to the work immediately and investigate your claim.

A Linear AC-OPF Formulation for Unbalanced Distribution Networks

Juan S. Giraldo *Member, IEEE*, Pedro P. Vergara *Member, IEEE*, Juan Camilo López *Member, IEEE*,
Phuong H. Nguyen *Member, IEEE*, and Nikolaos G. Paterakis *Member, IEEE*

Abstract—Linear optimal power flow (OPF) formulations are powerful tools applied to a large number of problems in power systems, e.g., economic dispatch, expansion planning, state estimation, congestion management, electricity markets, among others. This paper proposes a novel mixed-integer linear programming formulation for the AC-OPF of three-phase unbalanced distribution networks. The model aims to minimize the total energy production cost while guaranteeing the network's voltage and current magnitude operational limits. New approximations of the Euclidean norm, which is present in the calculation of nodal voltage and branch current magnitudes, are introduced by applying a linear transformation of weighted norms and a set of intersecting planes. The accuracy, optimality, feasibility, and scalability of the proposed linearizations are compared with common linear approximations in the literature using two unbalanced distribution test systems. The obtained results show that the proposed formulation is computationally more efficient (almost twice) while being as accurate and more conservative than the benchmarked approaches with maximum errors lower than 0.1%. Thus, its potential application in a variety of distribution systems operation and planning optimization problems is endorsed.

Index Terms—AC optimal power flow, unbalanced distribution networks, mixed-integer linear programming, Euclidean norm approximation.

NOMENCLATURE

Sets

Ω_B	Set of nodes
Ω_G	Set of nodes with distributed generation (DG) units
Ω_N	Set of intersecting planes for the current magnitude approximation.
Ω_R	Set of nodes with renewable energy source (RES)
Ω_T	Set of time periods
Ω_Φ	Set of phases $\{a, b, c\}$

Parameters

β	Coefficient for the voltage magnitude approx.
Δt	Duration of the time period t
λ	Coefficient for the voltage magnitude approx.
Θ	Range angle for the voltage magnitude approx.
\mathcal{T}_ϕ	Rotation coefficient for phase ϕ
c_g^{dg}	Unitary cost of energy at DG unit g

c_t^s	Unitary cost of energy at the substation at period t
$\bar{I}_{k,j}$	Maximum current magnitude at branch $k-j$
N	Number of intersecting planes current approx.
pf_g	Minimum operational power factor of DG unit g
\bar{P}_g	Maximum rated active power of DG unit g
$\mathbf{S}_{k,t}^{\text{id}}$	Vector of complex loads at node k , period t
$\mathbf{S}_{k,t}^{\text{re}}$	Vector of complex generation from the RES at node k , period t
\bar{V}	Maximum voltage magnitude
$\mathbf{V}_{k,t}^0$	Vector of estimated voltage at node k , period t
\underline{V}	Minimum voltage magnitude
$\mathbf{Y}_{k,j}$	Admittance submatrix between nodes $k-j$

Variables

$\Gamma_{k,j,t,\phi,n}$	Approximated current magnitude at branch $k-j$, period t , phase ϕ , intersecting plane n
$\Psi(z)$	Approximated Euclidean norm of vector z
$\mu_{g,t}$	Unit commitment of DG unit g , period t
$\mathbf{I}_{k,j,t}$	Vector of three-phase currents at branch $k-j$, period t
$\mathbf{I}_{g,t}^{dg}$	Vector of three-phase currents from the DG at node g , period t
$\mathbf{I}_{k,t}^{ld}$	Vector of three-phase currents from the loads at node k , period t
$\mathbf{I}_{w,t}^{re}$	Vector of three-phase currents from the RES at node w , period t
$\mathbf{I}_{k,t}^s$	Vector of three-phase currents from the substation at node k , period t
$P_{g,t}^{dg}$	Three-phase active power from the DG at node g , period t
$Q_{g,t}^{dg}$	Three-phase reactive power from the DG at node g , period t
$\mathbf{V}_{k,t}$	Vector of three-phase voltages at node k , period t

I. INTRODUCTION

SECURE and economic operation of power systems relies on accurate and efficient AC optimal power flow (AC-OPF) models. The objective of an AC-OPF is to obtain the optimal dispatch of controllable energy resources to optimize a given objective while satisfying technical, physical, and operational limits. For a long time, AC-OPF problems were exclusively focused on bulk transmission systems. However, the growing penetration of distributed energy resources (DERs) into electrical distribution systems has created the need for accurate and efficient AC-OPF models aimed at medium/low-voltage networks [1]. One of the main characteristics of

Juan S. Giraldo is with the Mathematics of Operations Research group, EEMCS faculty, University of Twente, Enschede 7522NB, The Netherlands. Pedro P. Vergara is with the Intelligent Electrical Power Grids (IEPG) group, Delft University of Technology, Delft 2628CD, The Netherlands. Juan C. López is with the School of Electrical and Computer Engineering, University of Campinas, Campinas, Brazil. Phuong H. Nguyen and Nikolaos G. Paterakis are with the Energy Systems group, Eindhoven University of Technology, Eindhoven, 5612AP, the Netherlands. emails: jnse@ieee.org, p.p.vergarabarrios@tudelft.nl, jclopeza@unicamp.br, {n.paterakis, p.nguyen.hong}@tue.nl .

such systems is that unbalances between phases are more pronounced than in high-voltage ones, mainly due to single and two-phase loads, single phase laterals, and untransposed lines [2]. Classical AC-OPF formulations are nonlinear, non-convex, optimization problems containing both continuous and discrete variables. Hence, they are classified into the mixed-integer nonlinear programming (MINLP) family [3]. Including three-phase models for branches, transformers, voltage regulators, and DERs increases the size of the problem and the complexity of finding optimal solutions in deterministic polynomial time, since MINLP models are NP-hard [4]. Although mixed-integer linear programming (MILP) problems share the same computational complexity class, their tractability and the existence of mature solvers have motivated the derivation of approximated/relaxed formulations of originally nonlinear problems for over six decades [5]. Furthermore, linearized AC-OPF formulations are preferred in multi-period setups with integer variables since the implementation of decomposition techniques, such as Benders cuts, are straightforward in linear problems [6].

Convex relaxation models have been proposed in the literature for the AC-OPF problem as summarized in [7], where classic formulations and recent advances are shown. Convex relaxations based on second-order cone programming (SOCP) have been proposed in [8] for reconfiguration problems, or in [9], where authors expose the conditions for obtaining an exact equivalent model in balanced distribution networks. A two-step algorithm composed of a MILP and a quadratically constrained programming approach is proposed in [10] for managing overloads in balanced distribution systems.

Linear OPFs were initially based on the DC power flow as in [11], where different techniques are analyzed. However, linear approximations make it possible to obtain AC-OPF models as in [12], for balanced networks, using binary expansion discretization and piecewise linear approximations. Authors in [13] propose a MILP approach to the AC-OPF for balanced three-phase radial systems including piecewise linear approximations of nonlinear functions. In [14], a linear AC-OPF model is proposed for AC-DC networks, and in [15] a MILP formulation is introduced. Notice that the works above do not consider unbalanced networks. However, unbalances are a natural consequence of line configurations, i.e., untransposed, two-phase and single-phase laterals, and load characteristics, where single-phase and two-phase connections prevail [16].

A three-phase AC-OPF for distribution systems is proposed in [17] and [18] as a semidefinite programming model disregarding integer variables or in [19] as a mixed-integer quadratically-constrained AC-OPF. Unbalanced linear formulations have also been used for different applications as in [20] for the optimal charging coordination of electric vehicles, in [17] and [19] as semidefinite relaxations, in [21] for the optimal operation of islanded microgrids, in [22] for optimal network restoration, or in [23] for short circuit analysis. However, these models show some drawbacks regarding their accuracy, optimality, feasibility, and/or scalability.

This paper proposes a novel MILP formulation for the AC-OPF problem of three-phase unbalanced distribution networks. The model aims to minimize the network's total operational

cost while guaranteeing voltage and current magnitude operational limits. The proposed formulation is an extension of the authors' previous work in [24], introducing a generalization of the methodologies and additional results. Specifically, the intersecting planes linearization for current magnitudes has been generalized, along with introducing a linear transformation to reduce the approximation error of voltage magnitudes. The proposed MILP model accounts for dispatchable distributed generation (DG) units, and it can be easily extended to include energy storage systems, on-load tap changers, voltage regulators, controllable capacitor banks, among other distribution automation devices. Hence, it could be applied to various problems in power systems by introducing the corresponding linearized models. The accuracy, optimality, feasibility, and scalability of the proposed linearizations have been compared to common approximations in the literature in two unbalanced distribution test systems with 25 and 123 nodes. Compared with similar works, the proposed formulation offers an improvement in the accuracy of the approximations with maximum errors lower than 0.1%, providing more conservative results (no violations of operational limits), and without scarifying computational efficiency. The main contributions of this paper are twofold:

- An accurate and scalable MILP model for the AC-OPF problem for unbalanced three-phase distribution systems that can be solved using commercial solvers.
- Two novel accurate linear approximations to the Euclidean norm in \mathbb{R}^2 that can be potentially applied in a wide variety of problems in power systems where magnitudes are involved, e.g., voltage, current, apparent power, distance, etc.

II. MIXED-INTEGER NONLINEAR PROGRAMMING MODEL

The MINLP model can be summarized in (1).

$$\begin{cases} \min f(\mathbf{V}, \mathbf{I}) & (2) \\ \text{s.t. } h(\mathbf{V}, \mathbf{I}) = 0 & (3)-(9) \\ g(\mathbf{V}, \mathbf{I}) \leq 0 & (10)-(14) \end{cases} \quad (1)$$

The proposed formulation minimizes the total energy production cost over a period of time, discretized in a finite number of time-steps $t \in \Omega_T$, each with a duration of Δt hours as shown in (2), where the first term relates the cost of importing energy from the main grid and the second one the operation cost of the DG units. Notice that a quadratic cost function could be linearized by using piece-wise linear approximations as in [21] or [25]. However, a linear function has been implemented for the sake of simplicity. The nodal current balance is expressed in complex form in (3), where $[\mathbf{Y}_{k,j}]$ is the (3×3) admittance submatrix of the branch connecting nodes k and j , both nodes belonging to the set of buses, i.e., $k, j \in \Omega_B$. It should be pointed out that some three-phase transformer connections may have numerical implications when dealing with the admittance matrix. Detailed transformer models can be found in [26]. Three-phase complex components are expressed by bold symbols, e.g., nodal voltages are expressed by the column vector $\mathbf{V}_{k,t} = [\mathbf{V}_{k,t,\phi}] = [v_{k,t,\phi}^r + jv_{k,t,\phi}^i]$ for all buses $k \in \Omega_B$,

all periods $t \in \Omega_T$, and all phases $\phi \in \Omega_\Phi$. Similarly, nodal complex currents injected by the substation, DG units, renewable sources, or loads are defined as $\mathbf{I}_{k,t}^x$, with x being the nature of the current injection.

For example, the current injected by the substation is identified as $x = s$, and must be set to zero for all buses but the substation bus (S), i.e., $\mathbf{I}_{k,t}^s = [0]$, $\forall k \in \Omega_B, t \in \Omega_T : i \neq S$. On the other hand, three-phase nodal voltages at the substation, which are used as reference, must be fixed as $\mathbf{V}_{k,t}^\top = [1, \alpha^2, \alpha]$ $\forall k \in \Omega_B, t \in \Omega_T : i = S$, where $\alpha = 1\angle 120^\circ$ hereinafter. Hence, the three-phase active power injected from the substation in (4) is a linear expression.

Loads are expressed as $\mathbf{S}_{k,t}^{ld}$ in (5), while injections from renewable sources are represented by $\mathbf{S}_{k,t}^{re}$ in (6). Total three-phase active and reactive powers injected by DG units are expressed in (7) and (8), respectively. Branch currents are defined as $\mathbf{I}_{k,j,t}$ in (9) and the maximum capacity of each branch in (10). The minimum and maximum voltage magnitude limit is considered in (11), while operational constraints regarding the capability curve of the DG units are considered in (12) and (13), and the ramp-up and ramp-down limits in (14).

$$f(\mathbf{V}, \mathbf{I}) = \sum_{t \in \Omega_T} \Delta t \left(\sum_{k \in \Omega_B} c_t^s P_{k,t}^s + \sum_{g \in \Omega_G} c_g^{dg} P_{g,t}^{dg} \right) \quad (2)$$

$$\mathbf{I}_{k,t}^s + \sum_{g \in \Omega_G: g=k} \mathbf{I}_{g,t}^{dg} + \sum_{w \in \Omega_R: w=k} \mathbf{I}_{w,t}^{re} - \mathbf{I}_{k,t}^{ld} = \sum_{j \in \Omega_B} \mathbf{Y}_{k,j} \mathbf{V}_{j,t}, \quad \forall k \in \Omega_B, t \in \Omega_T \quad (3)$$

$$P_{k,t}^s = \Re \left\{ \mathbf{V}_{k,t}^\top \mathbf{I}_{k,t}^{s*} \right\}, \quad \forall k \in \Omega_B, t \in \Omega_T : k = S \quad (4)$$

$$\mathbf{I}_{k,t}^{ld*} = \text{diag}(\mathbf{V}_{k,t})^{-1} \mathbf{S}_{k,t}^{ld}, \quad \forall k \in \Omega_B, t \in \Omega_T \quad (5)$$

$$\mathbf{I}_{k,t}^{re*} = \text{diag}(\mathbf{V}_{k,t})^{-1} \mathbf{S}_{k,t}^{re}, \quad \forall k \in \Omega_R, t \in \Omega_T \quad (6)$$

$$P_{g,t}^{dg} = \Re \left\{ \mathbf{V}_{g,t}^\top \mathbf{I}_{g,t}^{dg*} \right\}, \quad \forall g \in \Omega_G, t \in \Omega_T \quad (7)$$

$$Q_{g,t}^{dg} = \Im \left\{ \mathbf{V}_{g,t}^\top \mathbf{I}_{g,t}^{dg*} \right\}, \quad \forall g \in \Omega_G, t \in \Omega_T \quad (8)$$

$$\mathbf{I}_{k,j,t} = [\mathbf{Y}_{k,j}] (\mathbf{V}_{k,t} - \mathbf{V}_{j,t}), \quad \forall k, j \in \Omega_B, t \in \Omega_T : k \neq j \quad (9)$$

$$\|\mathbf{I}_{k,j,t}\|_2 \leq \bar{I}_{k,j}, \quad \forall k, j \in \Omega_B, t \in \Omega_T : k \neq j \quad (10)$$

$$\underline{V} \leq \|\mathbf{V}_{k,t}\|_2 \leq \bar{V}, \quad \forall k \in \Omega_B, t \in \Omega_T \quad (11)$$

$$\left| Q_{g,t}^{dg} \right| \leq P_{g,t}^{dg} \tan \left(\cos^{-1}(\text{pf}_g) \right), \quad \forall g \in \Omega_G, t \in \Omega_T \quad (12)$$

$$\mu_{g,t} \underline{P}_g \leq P_{g,t}^{dg} \leq \mu_{g,t} \bar{P}_g, \quad \forall g \in \Omega_G, t \in \Omega_T \quad (13)$$

$$\underline{P}_g^{\text{down}} \leq P_{g,t}^{dg} - P_{g,t-1}^{dg} \leq \bar{P}_g^{\text{up}}, \quad \forall g \in \Omega_G, t \in \Omega_T \quad (14)$$

where $\mu_{g,t} \in \{0, 1\}$ is a binary variable for the unit commitment of DG unit g at period t , and $\text{diag}(\cdot)$ represents a diagonal matrix containing the elements of the vector. Note that nonlinearities are introduced by the product between variables in (5)–(8), as well as by the calculation of current and voltage magnitudes in (10) and (11), respectively.

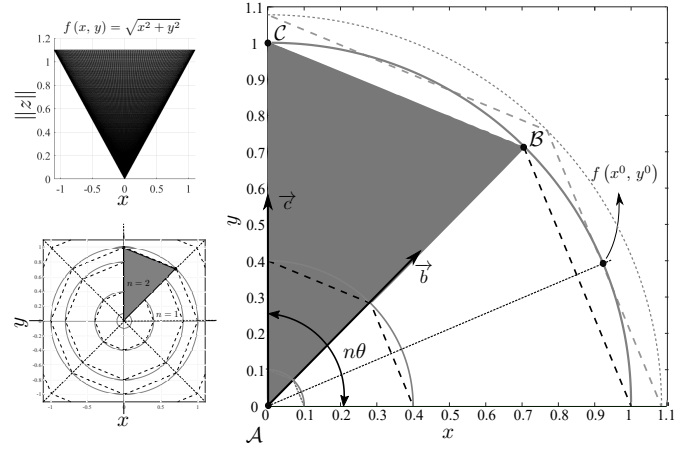


Fig. 1. Euclidean norm approximation using intersecting planes.

III. PROPOSED MILP MODEL

A. Linearization of Power Injections

A linear expression for (5) can be obtained using Taylor series expansion, evaluated on estimated/historical values for the real and imaginary parts of the nodal voltages, namely, $\mathbf{V}_{k,t}^0$. The first-order approximation is:

$$\mathbf{I}_{k,t,\phi}^{ld} \approx \mathbf{I}_{k,t,\phi}^{ld} \Big|_{\mathbf{V}_{k,t,\phi}^0} + \frac{\partial \mathbf{I}_{k,t,\phi}^{ld}}{\partial \mathbf{V}_{k,t,\phi}} \Big|_{\mathbf{V}_{k,t,\phi}^0} (\mathbf{V}_{k,t,\phi} - \mathbf{V}_{k,t,\phi}^0), \quad \forall k \in \Omega_B, t \in \Omega_T, \phi \in \Omega_\Phi \quad (15)$$

The error of these approximations depends on the estimated values $\mathbf{V}_{k,t}^0$. Furthermore, the accuracy of the first order linear approximation for injected power has been assessed considering voltage magnitude around 1.0 pu in [27]. These values can be set using an initial three-phase load flow analysis, experience-based values, or even a flat-start [22]. Similarly, (6)–(8) are approximated as:

$$\mathbf{S}_{k,t}^{re} \approx \mathbf{V}_{k,t}^0 \top \mathbf{I}_{k,t}^{re*}, \quad \forall k \in \Omega_R, t \in \Omega_T \quad (16)$$

$$P_{g,t}^{dg} \approx \Re \left\{ \mathbf{V}_{g,t}^0 \top \mathbf{I}_{g,t}^{dg*} \right\}, \quad \forall g \in \Omega_G, t \in \Omega_T \quad (17)$$

$$Q_{g,t}^{dg} \approx \Im \left\{ \mathbf{V}_{g,t}^0 \top \mathbf{I}_{g,t}^{dg*} \right\}, \quad \forall g \in \Omega_G, t \in \Omega_T \quad (18)$$

B. Proposed Approximation for Branch Current magnitudes

The Euclidean norm is defined as the root sum square of a vector. A new underestimate approximation to the Euclidean norm in \mathbb{R}^2 is proposed in this paper using intersecting planes. The proposed approximation is a generalization of the formulation in [28] for non-unitary norms. Take $z = \{x, y\}$ and $f(x, y) = \|z\|_2 \triangleq \sqrt{x^2 + y^2}$. Three non-collinear points, $\mathcal{A} = \{0, 0, 0\}$; $\mathcal{B}_n = \{\cos(\theta n - \theta), \sin(\theta n - \theta), 1\}$; $\mathcal{C}_n = \{\cos(n\theta), \sin(n\theta), 1\}$, are defined such as they belong to a set of intersecting planes with $f(x, y)$ for each plane $n \in \Omega_N$, where $\Omega_N = \{1, 2, \dots, N\}$ is the set of intersecting planes used to perform the approximation. A general representation of the approximation is shown in Fig. 1, where $\theta = 2\pi/N$ represents the angle between vectors

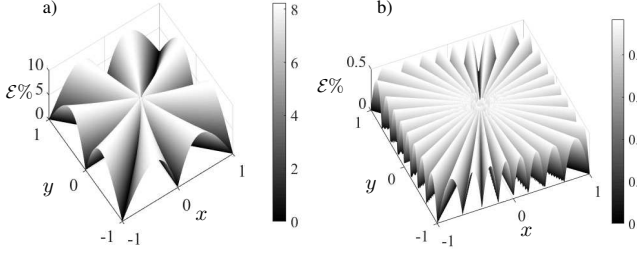


Fig. 2. Error of the Euclidean norm approximation – a) $N = 8$. b) $N = 32$.

\vec{b} & \vec{c} . With \vec{b} and \vec{c} it is possible to obtain planes $Z_n = \mathcal{AB}_n\mathcal{C}_n \forall n \in \Omega_N$, such as:

$$Z_n = (A_n x + B_n y) / C_n \quad (19a)$$

$$A_n = \sin(\theta n - \theta) - \sin(n\theta) \quad (19b)$$

$$B_n = \cos(n\theta) - \cos(\theta n - \theta) \quad (19c)$$

$$C_n = \cos(n\theta) \sin(\theta n - \theta) - \cos(\theta n - \theta) \sin(n\theta) \quad (19d)$$

A graphical representation of the error is shown in Fig. 2 for $N = \{8, 32\}$. It can be demonstrated that the maximum error at each plane n happens at $\theta^0 = \theta(2n - 1)/2$. For the sake of clarity, take $x^0 = \cos(\theta^0)$, $y^0 = \sin(\theta^0)$, and $n = 1$. An analytic expression for the maximum error at each intersecting plane as a function of N is obtained:

$$\bar{\mathcal{E}} = \left| 1 - \sec(\pi/N) \right| \quad (20)$$

It should be noted that (20) applies for each plane $n \in \Omega_N$ and it is valid for $\{x, y\} \in \mathbb{R}$.

Branch currents $\mathbf{I}_{k,j,t}$ are complex numbers. Thus, their magnitude is described as a Euclidean norm in \mathbb{R}^2 . After using the proposed approximation in (19), constraint (10) is transformed into (21) and (22).

$$\Gamma_{k,j,t,\phi,n} = \left(i_{k,j,t,\phi}^r A_n + i_{k,j,t,\phi}^i B_n \right) / C_n \quad (21)$$

$$\forall k, j \in \Omega_B, n \in \Omega_N, t \in \Omega_T, \phi \in \Omega_\Phi : k \neq j$$

$$\Gamma_{k,j,t,\phi,n} \leq \bar{\Gamma}_{k,j}, \quad (22)$$

$$\forall k, j \in \Omega_B, n \in \Omega_N, t \in \Omega_T, \phi \in \Omega_\Phi : k \neq j$$

Note that (21) is not the actual value of the branch current magnitude. Instead, it returns a value for each plane n that must satisfy the inequality constraints in (22). Thus, guaranteeing current limits. However, the approximated value of the current magnitude can be obtained by $\|\mathbf{I}_{k,j,t,\phi}\|_2 \approx \max_{n \in \Omega_N} \{\Gamma_{k,j,t,\phi,n}\}$ if needed. Furthermore, the proposed linearization can be applied in other models that involve norm limits, e.g., maximum apparent power of devices, distance constraints in routing problems, etc.

C. Proposed Approximation for Nodal Voltage Magnitudes

In principle, the approximation in Sec. III-B could also be applied for voltage magnitudes. However, from (20), it can be seen that the approximation error is proportional to N , increasing the computational burden if low errors are required. This paper proposes using specific regression parameters and

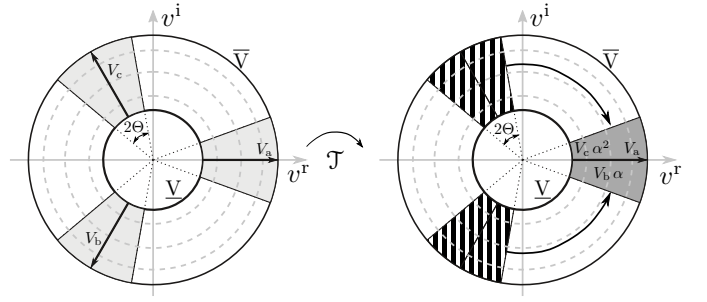


Fig. 3. Representation of rotated voltage magnitudes, limits, and range angle Θ .

a limited angle range for linearizing nodal voltage magnitudes. As stated in [29], any norm on \mathbb{R}^n can be approximated as a positive linear combination of other norms. The linearization approximates the Euclidean norm, $\|z\|_2$, as a linear combination of the $\|z\|_1$ norm and the $\|z\|_\infty$ norm. By definition, $\|z\|_\infty \leq \|z\|_2 \leq \|z\|_1$. Hence, it is possible to approximate $\|z\|_2$ as a linear combination of the other two:

$$\|z\|_2 \approx \Psi(z) = \lambda \|z\|_\infty + \beta \|z\|_1, \quad \lambda, \beta \geq 0 \quad (23)$$

where $\|z\|_\infty \triangleq \max\{|x|, |y|\}$ and $\|z\|_1 \triangleq |x| + |y|$. Using (23), voltage magnitudes are approximated as:

$$\Psi(V_{k,t,\phi}) = \lambda_\phi \|V_{k,t,\phi}\|_\infty + \beta_\phi \|V_{k,t,\phi}\|_1 \quad (24)$$

$$\forall k \in \Omega_B, t \in \Omega_T, \phi \in \Omega_\Phi$$

with $V_{k,t,\phi} = v_{k,t,\phi}^r + jv_{k,t,\phi}^i$. Due to power quality standards, distribution systems are designed such as voltages are close to nominal values under normal operation, i.e., magnitudes within 0.90–1.10 pu, phase angles deviations as small as possible, and a voltage unbalance factor lower than 5% [30]. Thus, a nonnegative angle range, namely Θ , is introduced to tighten up the approximation. This range must contain system's voltage phase deviations, as depicted in Fig. 3, where $V_a = 1$, $V_b = \alpha^2$, and $V_c = \alpha$, represent phase nominal voltages.

The quality of the approximation in (24) relies on using suitable values for λ_ϕ and β_ϕ , which can be obtained using regression techniques. These coefficients are a function of Θ and are independent of the voltage magnitude, as shown in [24] where 10,000 randomly generated samples were used for the regressions. Notice that no additional power flows must be performed in this step. However, the main drawback of the formulation in [24] corresponds to the errors for $\phi = \{b, c\}$, which are approximately five times greater than errors for $\phi = \{a\}$. The reason for this drawback has been explained in [24], highlighting the location of each phase in the complex plane as the main cause.

A new formulation is proposed in this paper to reduce the approximation error for $\phi = \{b, c\}$ by performing a linear rotation to the voltages as depicted in Fig. 3. A similar approach was performed in [31], for different purposes. In our paper, the rotation reduces the maximum expected error of the approximation for $\phi = \{b, c\}$ to the same levels obtained for $\phi = \{a\}$. The maximum approximation errors are shown in Fig. 4a for $\phi = \{b, c\}$ before and after the rotation as a function of Θ . It can be seen that the maximum expected error

after performing the rotation is 0.58% at $\Theta = 15^\circ$, which is approximately four times lower than without performing the rotation (2.3%). Fitting functions are displayed in the figure with an obtained coefficient of determination $r^2 > 0.97$.

Notice that performing the rotation also reduces the number of required parameters, i.e., $\lambda_a = \lambda_b = \lambda_c = \lambda$ and $\beta_a = \beta_b = \beta_c = \beta$. Furthermore, after 10,000 samples, it was found that λ and β follow a quasi-linear relationship within the range of interest, $0^\circ < \Theta \leq 15^\circ$, as can be seen in Fig. 4b where the fitting functions for parameters λ and β are displayed with an obtained coefficient of determination $r^2 > 0.99$.

Once the parameters of the linearization are defined, the operational constraints for voltage magnitudes in (11) can be rewritten as:

$$\underline{V} \leq \Psi(\mathcal{V}_{k,t,\phi}) \leq \bar{V}, \quad \forall k \in \Omega_B, t \in \Omega_T, \phi \in \Omega_\Phi \quad (25)$$

where $\mathcal{V}_{k,t,\phi}$ are the rotated voltages, i.e., $\mathcal{V}_{k,t,\phi} = V_{k,t,\phi} \mathcal{T}_\phi$, and $\mathcal{T}_\phi = \{1, \alpha, \alpha^2\}$ are the rotation coefficients. Notice that $\Re\{\mathcal{V}_{k,t,\phi}\} \geq 0$. Hence, $|\Re\{\mathcal{V}_{k,t,\phi}\}| = \Re\{\mathcal{V}_{k,t,\phi}\}$. Furthermore, since $\Re\{\mathcal{V}_{k,t,\phi}\} > \Im\{\mathcal{V}_{k,t,\phi}\}$ for $\Theta < 45^\circ$, then, $\|\mathcal{V}_{k,t,\phi}\|_\infty = \Re\{\mathcal{V}_{k,t,\phi}\}$. Therefore, (24) is rewritten as:

$$\Psi(\mathcal{V}_{k,t,\phi}) = \lambda \Re\{\mathcal{V}_{k,t,\phi}\} + \beta \left(\Re\{\mathcal{V}_{k,t,\phi}\} + |\Im\{\mathcal{V}_{k,t,\phi}\}| \right), \quad \forall k \in \Omega_B, t \in \Omega_T, \phi \in \Omega_\Phi \quad (26)$$

It should be pointed out that the proposed rotation does not modify the rectangular components of the nodal voltages in any other constraint of the model. The rotation is performed only for the voltage operational limit constraints. Furthermore, the accuracy of the proposed voltage magnitude linearization is only dependant on Θ ; thus, it is perfectly scalable.

D. Obtained MILP Model

The obtained MILP model can be summarized in (27).

$$\begin{cases} \min & (2) \\ \text{s.t.} & (3), (4), (9), (12)\text{--}(18), \\ & (21), (22), (25), (26) \end{cases} \quad (27)$$

IV. TEST CASES

A. Case I - Assessment of Accuracy, Optimality, and Feasibility

An unbalanced 25-bus test system has been used for testing the accuracy, optimality, and feasibility of the proposed model.

TABLE I
VALUES AND UNITS OF PARAMETERS.

	Parameter	Value	Unit
DG units	c^{dg}	0.04	\$/kWh
	pf	0.9	—
	\bar{P}	700	kW
	$\bar{P}^{\text{up}} = -\bar{P}^{\text{dwn}}$	350	kW
System	c^s	0.03	\$/kWh
	\bar{I}	530	A
	\bar{V}	1.05	pu
	\underline{V}	0.95	pu

All system branches are three-phase with three conductors and only one line-to-line voltage level (4.16 kV). All loads are three-phase, and some of them are unbalanced. Topology, lines' parameters, and loads nominal data can be found in [32]. Three DG units have been added to the original system at buses 13, 19, and 25. DG units' parameters and system information can be found in Table I. Without loss of generality, parameters for DGs and maximum current magnitude limits have been arbitrarily chosen and are the same for all the DG units and feeders, respectively. The problem has been solved for $\Omega_T = \{1, 2, \dots, 5\}$ with different operating points. Results were obtained using the proposed MILP model, containing the introduced linearizations for voltage and current magnitudes, and benchmarked with other linearization techniques for the Euclidean norm applied to power systems. State variables were compared to those found using a conventional power flow after fixing the obtained power injections. These power injections are the results from dispatchable DG units and were obtained for each tested linearization technique. The flow chart of the comparison process is shown in Fig. 5.

All linearization techniques have been implemented in the modelling language AMPL [33] and solved with CPLEX [34]. Due to the lack of real measurements, the results from a traditional power flow have been used as initial estimated values. However, in practical implementations, recent SCADA measurements could also be used if they are available.

The computational burden for solving the models has been measured in terms of *ticks* and seconds. Ticks are consistent measures of computational burden independent of the concurrent load of the workstation. It is also considered fairer than comparing only time since the ratio of ticks per second stays roughly constant for the same platform and the same load, independent of the model solved [34].

1) *Current magnitudes*: Three techniques were used to compare the approximation for current magnitudes: *A1* is an approximation with intersecting planes and a fixed accuracy, as in [24]; *A2* is a pure piecewise linearization in which the accuracy depends on the number of blocks, B as in [12], [13], [20]; and *A3*, where the polyhedral ϵ -approximation is proportional to parameter ν , as in [8]. On a first test, only current magnitude limits were enforced using the aforementioned techniques, disregarding voltage magnitude limits. The proposed formulation was tested using $N = \{12, 24, 32, 64\}$, while parameters for *A2* and *A3* are shown in Table II. The accuracy of the tested approximations can be contrasted in Table II by the mean squared error (MSE) and the maximum error between the obtained results and a conventional power flow. Phase current magnitudes at branch 1–2 are plotted in Fig. 6 using the proposed approximation with $N = 32$ and *A3* with $\nu = 4$. Branch 1–2 is prone to overcurrents because it connects the substation to the rest of the distribution system.

Regarding the feasibility of the tested techniques, it can be seen that the proposed approximation is always lower than the maximum magnitude limit independently of the number of cutting planes. This result was expected since the proposed formulation was deduced as an underestimate of the Euclidean norm, asymptotically approaching the actual current magnitude as N increases. In other words, the proposed

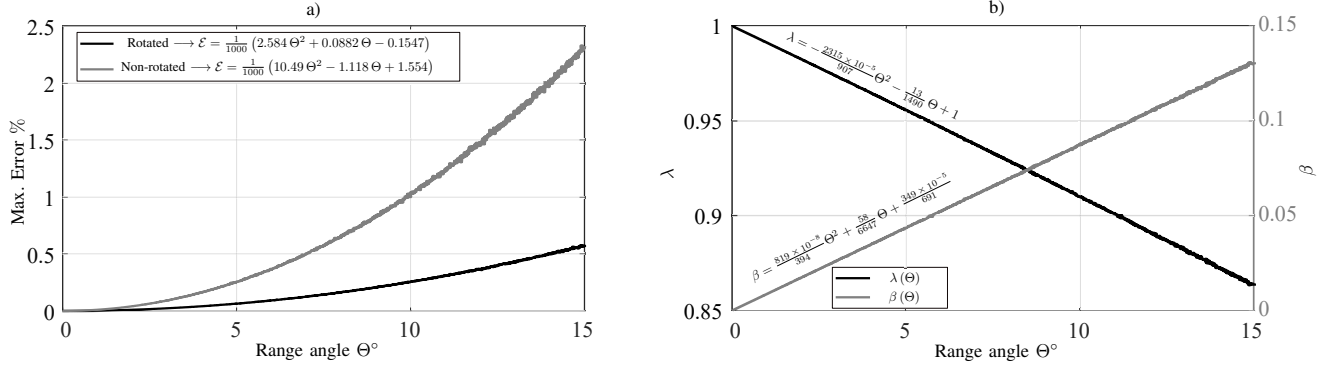


Fig. 4. Voltage magnitude approximation – a) Maximum error. b) Linearization parameters.

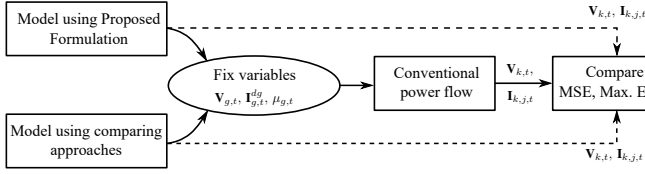


Fig. 5. Chart flow of the approximation comparison.

approximation will always provide a conservative solution as long as it is feasible. On the other hand, the techniques used for comparison (A1, A2, and A3) are not able to guarantee the current magnitude limit, providing solutions that can be infeasible in terms of current limits.

The computational burden of the proposed techniques can be compared in Table II. One can see that the computational burden and the accuracy of the approximation are indirectly proportional. In the case of the proposed formulation, it is due to the increasing number of constraints and variables with the number of intersecting planes. However, the maximum error stabilizes around 0.45% for $N \geq 32$. This error is linked to other linearizations within the model, such as the linearization of power injections. Note that the proposed approximation provides satisfactory results with a lower computational burden compared to the other tested techniques. In the case of A2 and A3, the accuracy of the solution is also adjustable. However, as previously discussed, the feasibility of the original problem cannot be guaranteed.

TABLE II
COMPARISON OF TECHNIQUES FOR CURRENT MAGNITUDE APPROXIMATION.

Technique	Parameter	MSE [%]	Max. Error [%]	Max. $\ I\ $ [A]	Ticks	Time [s]
Proposed	$N = 12$	45.64 E-3	1.7619	517.03	150.24	0.23
	$N = 24$	4.83 E-3	0.5272	525.96	393.10	0.47
	$N = 32$	2.38 E-3	0.4547	529.91	558.03	0.72
	$N = 64$	1.97 E-3	0.4547	529.95	1030.98	1.29
A1 [24]	–	15.73 E-3	2.5543	532.03	327.24	0.38
A2 [20]	$B = 4$	2.27 E-3	0.4913	529.88	811.85	1.16
	$B = 8$	2.25 E-3	0.4781	530.83	1116.13	1.65
	$B = 16$	2.12 E-3	0.4547	530.20	2384.59	4.49
A3 [8]	$\nu = 4$	317.9 E-3	1.2792	539.88	727.28	1.29
	$\nu = 6$	7.81 E-3	0.4678	530.61	970.72	1.54
	$\nu = 8$	2.00 E-3	0.4638	530.03	1035.33	1.64

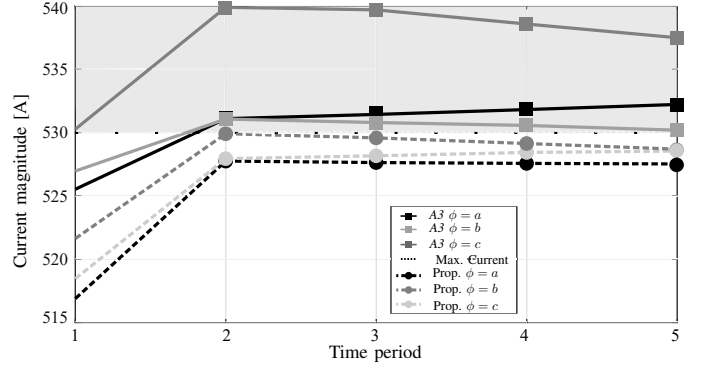


Fig. 6. Current magnitudes with two different techniques – $N = 32$ and A3 with $\nu = 4$.

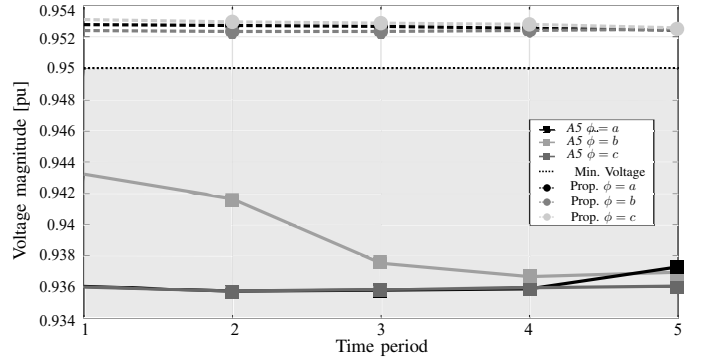


Fig. 7. Voltage magnitudes with two different techniques – $\Theta = 10^\circ$ and A5 with $\theta_+ = 10^\circ$.

2) *Voltage magnitudes*: Two different techniques were used to compare the approximation for voltage magnitudes. Approximation A4 is controlled by the same range angle used in the proposed formulation, Θ , but without the introduced rotation [24]. While approximation A5 uses a geometrical representation driven by θ_+ , as in [22]. Only voltage magnitude limits were enforced using the techniques mentioned earlier, while current magnitude limits were disregarded in this test case. The proposed formulation was tested using $\Theta = \{1, 5, 10\}^\circ$, and the corresponding values for A5, as shown in Table III. The accuracy of the tested approximations can be contrasted in Table III by the MSE and the maximum error between the obtained results and a conventional power

flow.

Phase voltage magnitudes at bus 15 are plotted in Fig. 7 using the proposed approximation with $\Theta = 10^\circ$ and A5 with $\theta_+ = 10^\circ$. Bus 15 is prone to undervoltages since it presents the lowest voltage of the system. One can see that the proposed approximation obtains results that remain within the specified voltage magnitude limits, providing feasible results. This result is true even when the approximation accuracy is compromised, i.e., when Θ increases. On the other hand, as shown in Table III, neither A4 nor A5 are able to guarantee the lower voltage limit constraint, which leads to infeasible solutions. Moreover, the errors are lower when using the proposed approach, requiring comparable computational times with the other tested techniques.

It should be stated that the accuracy of approximation A5 is highly sensitive to the value of θ_+ , as can be seen in Table III. Furthermore, due to the way it has been formulated, a wrong setting of this parameter may lead to infeasibility. For example, when θ_+ is lower than the maximum angle deviation of the system. On the other hand, although the proposed formulation's accuracy is also dependent on how close Θ is to the maximum deviation, a wrong estimation of the range angle does not mean instantaneous infeasibility, as it does in A5. In particular, for the tested system, the maximum angle deviation was lower than 1° for all phases, which upholds why all tested techniques behaved outstandingly in terms of accuracy and feasibility for $\Theta = \theta_+ = 1^\circ$.

The computational burden shows a dependency on the range angle. However, this is not caused by an increase in the number of constraints or variables as in current magnitudes. The variation in computational times depends on the number of internal iterations required by the solver to converge, which is directly related to the error induced by the approximations.

The value of the objective function obtained with different combinations of the linearization techniques is shown in Fig. 8. The value of the objective function is shown for the proposed formulation using $N = 32$ and different values of Θ . Results are compared with a combination between A3×A4, and the combination between A3×A5. The linearization parameter has been set to $\nu = 6$ for A3. Similarly, the total energy injected by all DG units and the substation is plotted in Fig. 9.

In Fig. 9, it can be seen that the sharing on the injected energy differs according to the approximation technique as the range angle increases. These differences are translated into

TABLE III
COMPARISON OF TECHNIQUES FOR VOLTAGE MAGNITUDE APPROXIMATION.

Technique	Parameter	MSE [%]	Max. Error [%]	Min. $\ V\ $ [pu]	Ticks	Time [s]
Proposed	$\Theta = 1^\circ$	1.29 E-9	0.0280	0.9500	176.97	0.26
	$\Theta = 5^\circ$	6.79 E-8	0.0688	0.9505	185.41	0.29
	$\Theta = 10^\circ$	6.51 E-7	0.2866	0.9524	200.43	0.32
A4 [24]	$\Theta = 1^\circ$	1.69 E-9	0.0266	0.9500	244.70	0.27
	$\Theta = 5^\circ$	9.42 E-8	0.2434	0.9489	299.70	0.33
	$\Theta = 10^\circ$	8.56 E-6	1.0227	0.9451	324.37	0.37
A5 [22]	$\theta_+ = 1^\circ$	1.39 E-9	0.0452	0.9498	187.94	0.23
	$\theta_+ = 5^\circ$	3.75 E-8	0.0512	0.9465	190.01	0.22
	$\theta_+ = 10^\circ$	2.03 E-7	0.1264	0.9357	196.48	0.23

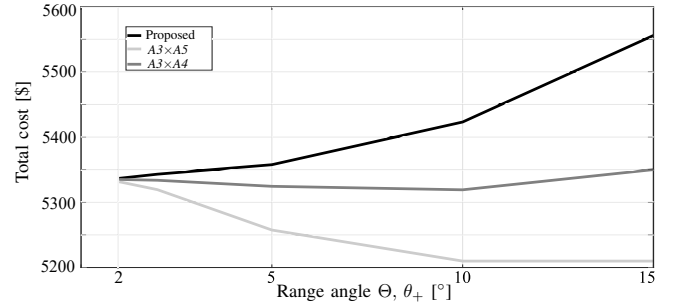


Fig. 8. Objective function cost using different techniques as a function of the range angle.

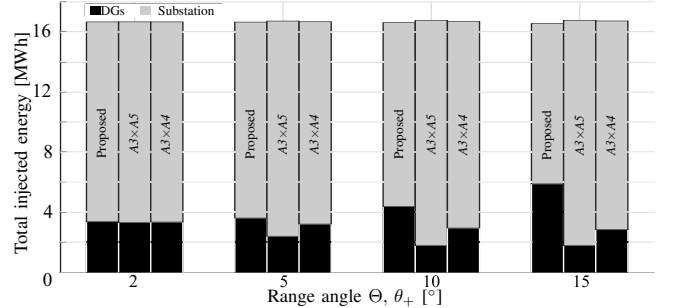


Fig. 9. Total injected energy from DG units and the substation.

variations on the total cost in Fig. 8, with a clear tendency of the proposed formulation to provide more expensive solutions whereas A3×A5 the cheapest. Note that the tested techniques got similar results for $\Theta = \theta_+ = 2^\circ$, but differ as the range angle increases. At the same time, the accuracy of the approximations decreases with the angle, and the feasibility of the original nonlinear problem can be compromised depending on the used technique. Furthermore, the proposed model's solution has been shown to be more conservative, i.e., both voltage and current limits are guaranteed irrespective of the value of Θ or N , providing feasible solutions to the original nonlinear problem. This conclusion is based on the differences in power dispatches and the performed accuracy/feasibility analyses. In other words, cost differences between techniques can be interpreted as the cost of increasing the feasibility and accuracy of the approximations.

B. Case II - Scalability and Sensitivity to Unbalance level

The three-phase IEEE 123-node test feeder has been used in this section to show the scalability of the proposed formulation. The substation transformer is a 5 MVA, 115/4.16 kV solidly-grounded wye, and it is located at bus 115. The system counts with overhead and underground lines with single-phase, two-phase, and three-phase branches feeding spot loads, with phase *a* being the most loaded one (around 1.4 MW at peak hour) and phase *b* the lightest one (around 0.89 MW at peak hour). Some modifications were made to emphasize the paper's focus; for example, voltage regulators, reactive power compensators, and transformer vector groups were disregarded. Detailed characteristics can be found in [35].

A planning horizon of 24 periods has been used, resembling an hourly day-ahead dispatch while loads have been scaled

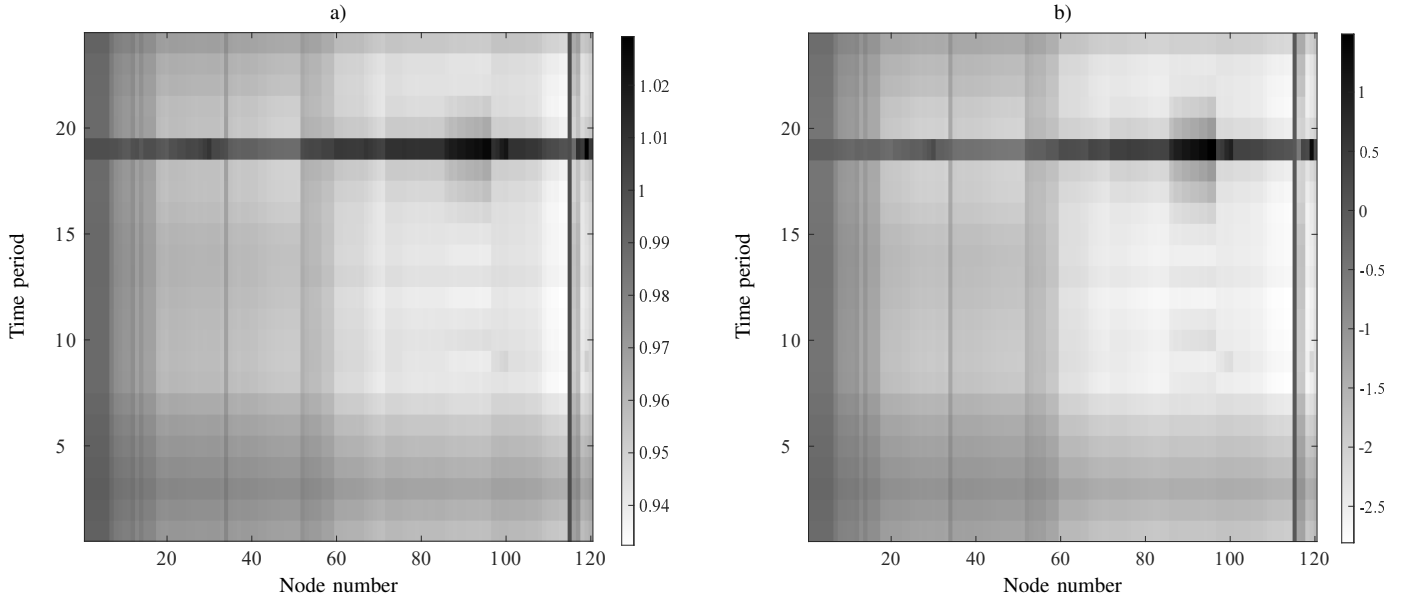


Fig. 10. Case II, $unb = 1$ - a) Voltage magnitudes at phase a . b) Voltage phase angles at phase a .

following a standard daily load curve. Three DG units were added to the original system with minimum and maximum power of $\underline{P} = 150$ kW and $\bar{P} = 1.5$ MW, respectively, and a minimum power factor of $pf = 0.9$. The DG units were connected at buses 117, 119, and 120, representing the interconnection with other feeders in the original network. The maximum current magnitude of all branches has been set to $\bar{I} = 500$ A and voltage magnitude limits to $\underline{V} = 0.90$ pu and $\bar{V} = 1.10$ pu.

The proposed formulation's scalability is shown by using an optimization problem more than twenty times bigger than the one used in Section IV-A with a total of 52,080 variables. The execution time as a function of the number of binary variables has been assessed by including additional DG units. Results are displayed in Fig. 11, where the execution times for different values of Θ are shown. It can be seen that the execution time increases with the number of binary variables, as expected in MILP problems.

The sensitivity of the proposed formulation to the network's unbalance level is assessed by increasing the total load of one of the phases. All nominal loads connected to phase a have been scaled by a factor, namely unb , where $unb = 1.0$ stands for the base case. For all tested cases, the range angle has been set to $\Theta = 2^\circ$, while the number of cutting planes to $N = 32$. Voltage magnitudes and phase angles at phase a for the base case are displayed in Fig. 10 for reference. Notice that the highest voltages occur at period 19, coinciding with the peak load of the system. This behaviour happens due to the power contribution from DGs to satisfy operational constraints.

Obtained results are shown in Table IV, where the execution time of the base case can be seen in the first row ($unb = 1.0$), with an average of 13.48 s. Additional tests, identified by *, were performed using different values for Θ . Maximum percent errors for different unbalance levels are shown in Table IV, where the maximum approximation errors of voltage and current magnitudes are displayed. The obtained

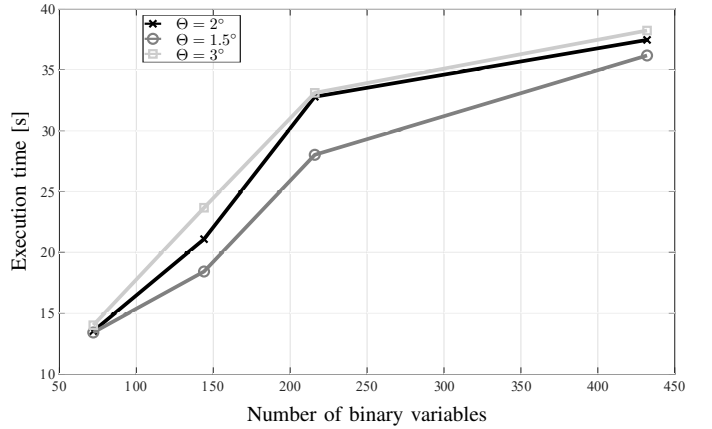


Fig. 11. Execution time as a function of the number of binary variables for different values of Θ .

objective function was compared by solving the non-linear programming problem in (1) after relaxing the integrality. Errors for voltage and current magnitudes increase with the unbalance level, as well as the error of the objective function value obtained with the proposed method. Voltage errors range from 0.02% to 0.22% while current errors from 0.83% to 1.41% for a load increase of 65%, only in one phase. The voltage unbalance level has been calculated using sequence components with a maximum unbalance of 2.98%. Higher values were not included since they lead to computational infeasibility.

Maximum percentage errors for voltage magnitudes as a function of the loading unbalance levels are shown in Fig. 12a for the tested time periods. It can be seen that the obtained approximation errors have a similar tendency depending on the time period due to the loading curve. However, the main reason causing the error increase is related to the angle deviations of each phase. Figure 12b displays the maximum absolute angle deviation from their nominal values (0° , -120° , 120°) of all

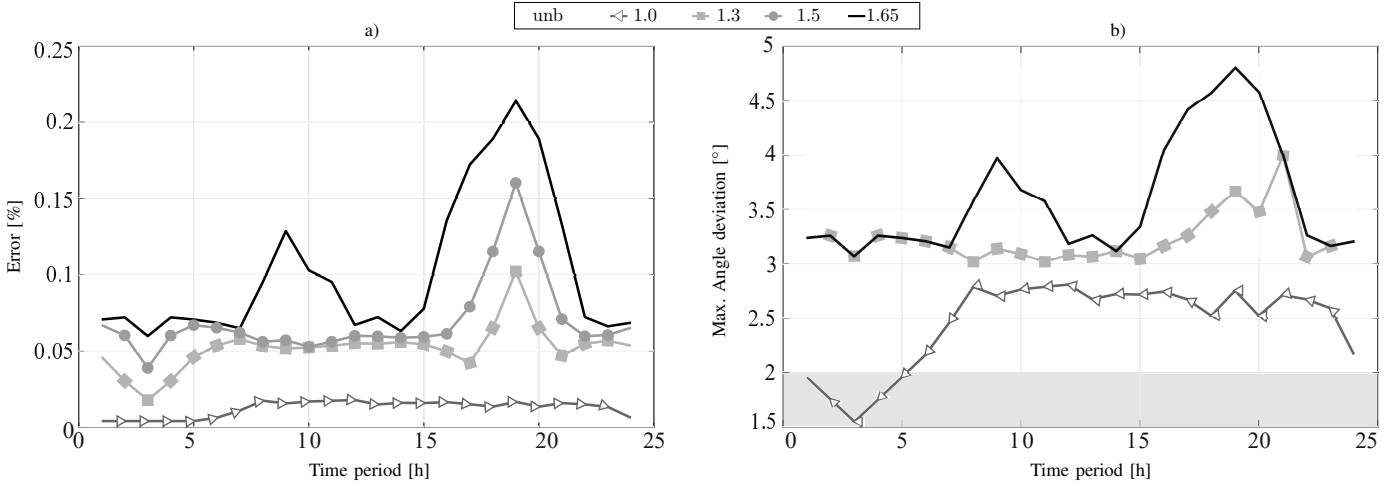


Fig. 12. a) Maximum voltage magnitude error as a function of network’s imbalance. b) Maximum absolute phase angle deviation from its nominal value as a function of network’s imbalance.

phases at all nodes. It can be seen that the approximation error increases as the deviation angle stray from the selected range angle, i.e., from $\Theta = 2^\circ$ in this case.

As explained in Section III-C, using a proper value for parameter Θ reduces the expected approximation error; this is, the range angle must be bigger than or equal to the maximum angle deviation of the system. This statement is corroborated in Table IV marked by *, $\text{unb} = \{1.0^*, 1.3^*, 1.5^*, 1.65^*\}$, where the errors using $\Theta = \{3^\circ, 4^\circ, 4.5^\circ, 5^\circ\}$ are shown, respectively. It can be seen that, in the worst case, errors are reduced by at least 1.5 times, e.g., from 1.4077% to 0.8951%, just by using a proper range angle value.

V. CONCLUSIONS

A novel linear AC-OPF model for three-phase unbalanced distribution networks considering binary variables was proposed in this paper. The original MINLP problem has been derived as an approximated MILP, aiming to minimize the network’s energy cost respecting operational constraints. Two novel linearizations for nodal voltage and branch current magnitudes were introduced showing their accuracy and scalability, indicating their potential application to a variety of problems in power systems.

The proposed formulation was compared regarding its accuracy, optimality, and feasibility with five different linearizations for voltage and current magnitudes available in

the literature. Results showed improvements in accuracy and computational burden, providing conservative results in terms of feasibility for different values of Θ and N . The optimality was also assessed with a nonlinear power flow after fixing the power injections, showing satisfactory results; while the model’s scalability was evident after using different size networks. A sensitivity analysis was performed regarding the accuracy of the linearized model to different unbalance levels. Results showed that errors increased under incorrect estimations of Θ when the maximum angle deviation of the system increases. However, it was shown that setting an appropriate value for the range angle reduces considerably the maximum approximation error.

REFERENCES

- [1] J. A. Momoh, M. E. El-Hawary, and R. Adapa, “A review of selected optimal power flow literature to 1993. II. Newton, linear programming and interior point methods,” *IEEE Trans. Power Syst.*, vol. 14, no. 1, pp. 105–111, Feb. 1999.
- [2] J. S. Giraldo, J. C. López, J. A. Castrillon, M. J. Rider, and C. A. Castro, “Probabilistic OPF Model for Unbalanced Three-Phase Electrical Distribution Systems Considering Robust Constraints,” *IEEE Trans. Power Syst.*, vol. 34, no. 5, pp. 3443–3454, Sep. 2019.
- [3] S. Frank, I. Steponavice, and S. Rebennack, “Optimal power flow: a bibliographic survey I,” *Energy Systems*, vol. 3, no. 3, pp. 221–258, Apr. 2012.
- [4] P. Belotti, C. Kirches, S. Leyffer, J. Linderoth, J. Luedtke, and A. Mahajan, “Mixed-integer nonlinear optimization,” *Acta Numerica*, vol. 22, pp. 1–131, May 2013.
- [5] J. P. Vielma, “Mixed integer linear programming formulation techniques,” *Siam Review*, vol. 57, no. 1, pp. 3–57, Apr. 2015.
- [6] A. M. Geoffrion, “Generalized Benders decomposition,” *Journal of optimization theory and applications*, vol. 10, no. 4, pp. 237–260, Oct. 1972.
- [7] F. Zohrizadeh, C. Jozs, M. Jin, R. Madani, J. Lavaei, and S. Sojoudi, “A survey on conic relaxations of optimal power flow problem,” *Eur. J. Oper. Res.*, vol. 287, no. 2, pp. 391 – 409, Dec. 2020.
- [8] R. A. Jabr, R. Singh, and B. C. Pal, “Minimum Loss Network Reconfiguration Using Mixed-Integer Convex Programming,” *IEEE Trans. Power Syst.*, vol. 27, no. 2, pp. 1106–1115, May 2012.
- [9] M. Nick, R. Cherkaoui, J. L. Boudec, and M. Paolone, “An exact convex formulation of the optimal power flow in radial distribution networks including transverse components,” *IEEE Trans. Autom. Control*, vol. 63, no. 3, pp. 682–697, Mar. 2018.

TABLE IV

APPROXIMATION ERRORS UNDER DIFFERENT PHASE UNBALANCE LEVELS.

unb	Unb. Level [%]	Max. Error V [%]	Max. Error I [%]	Obj. Error [%]	Time [s]
1.0		0.0176	0.8260	0.1165	13.48
1.0*	1.39	0.0095	0.5408	0.0685	13.99
1.3		0.1021	1.0501	0.3757	22.08
1.3*	2.03	0.0293	0.6141	0.0881	23.11
1.5		0.1601	1.2205	0.4598	18.44
1.5*	2.53	0.0480	0.8138	0.1148	20.02
1.65		0.2146	1.4077	0.7598	18.65
1.65*	2.98	0.0628	0.8951	0.1202	19.87

- [10] F. Capitanescu and I. Bilibin, "A tractable two-step MILP-QCP approach to on-line thermal constraint management in large radial active distribution systems," *Electr. Power Syst. Res.*, vol. 140, pp. 580–587, Nov. 2016.
- [11] Z. Yang, H. Zhong, Q. Xia, and C. Kang, "Solving OPF using linear approximations: fundamental analysis and numerical demonstration," *IET Gener. Transm. Dis.*, vol. 11, no. 17, pp. 4115–4125, Dec. 2017.
- [12] T. Akbari and M. Tavakoli Bina, "Linear approximated formulation of AC optimal power flow using binary discretisation," *IET Gener. Transm. Dis.*, vol. 10, no. 5, pp. 1117–1123, Apr. 2016.
- [13] R. S. Ferreira, C. L. T. Borges, and M. V. F. Pereira, "A Flexible Mixed-Integer Linear Programming Approach to the AC Optimal Power Flow in Distribution Systems," *IEEE Trans. Power Syst.*, vol. 29, no. 5, pp. 2447–2459, Feb. 2014.
- [14] H. Ergun, J. Dave, D. Van Hertem, and F. Geth, "Optimal Power Flow for AC-DC Grids: Formulation, Convex Relaxation, Linear Approximation, and Implementation," *IEEE Trans. Power Syst.*, vol. 34, no. 4, pp. 2980–2990, Jul. 2019.
- [15] M. Nozarian, A. H. Nikoofard, and A. Fereidunian, "Efficient MILP formulations for AC optimal power flow to reduce computational effort," *Int. T. on Electr. Energy*, Mar. 2020.
- [16] J. S. Giraldo, J. A. Castrillon, C. A. Castro, and F. Milano, "Optimal Energy Management of Unbalanced Three-Phase Grid-Connected Microgrids," in *2019 IEEE Milan PowerTech*, Milan, Italy, 2019.
- [17] L. Gan and S. H. Low, "Convex relaxations and linear approximation for optimal power flow in multiphase radial networks," in *2014 Power Systems Computation Conference*, Wroclaw, Poland, 2014.
- [18] Y. Liu, J. Li, and L. Wu, "ACOPF for three-phase four-conductor distribution systems: semidefinite programming based relaxation with variable reduction and feasible solution recovery," *IET Gener. Transm. Dis.*, vol. 13, no. 2, pp. 266–276, Jan. 2019.
- [19] L. Gutierrez-Lagos, M. Z. Liu, and L. F. Ochoa, "Implementable Three-Phase OPF Formulations for MV-LV Distribution Networks: MILP and MIQCP," in *2019 IEEE PES Innovative Smart Grid Technologies Conference - Latin America*, Gramado, Brazil, 2019.
- [20] J. F. Franco, M. J. Rider, and R. Romero, "A mixed-integer linear programming model for the electric vehicle charging coordination problem in unbalanced electrical distribution systems," *IEEE Trans. Smart Grid*, vol. 6, no. 5, pp. 2200–2210, Sep. 2015.
- [21] P. P. Vergara, J. C. López, M. J. Rider, and L. C. P. da Silva, "Optimal operation of unbalanced three-phase islanded droop-based microgrids," *IEEE Trans. Smart Grid*, vol. 10, no. 1, pp. 928–940, Jan 2019.
- [22] J. C. López, J. F. Franco, M. J. Rider, and R. Romero, "Optimal restoration/maintenance switching sequence of unbalanced three-phase distribution systems," *IEEE Trans. Smart Grid*, vol. 9, no. 6, pp. 6058–6068, Nov 2018.
- [23] F. Geth, S. Claeys, and G. Deconinck, "Current-Voltage Formulation of the Unbalanced Optimal Power Flow Problem," in *2020 8th Workshop on Modeling and Simulation of Cyber-Physical Energy Systems*, Sydney, Australia, 2020.
- [24] J. S. Giraldo, P. P. Vergara, J. C. López, P. H. Nguyen, and N. G. Paterakis, "A Novel Linear Optimal Power Flow Model for Three-Phase Electrical Distribution Systems," in *2020 Int. Conf. on Smart Energy Systems and Technologies (SEST)*, Istanbul, Turkey, 2020.
- [25] Z. Yang, H. Zhong, Q. Xia, and C. Kang, "Solving OPF using linear approximations: fundamental analysis and numerical demonstration," *IET Gener. Transm. Dis.*, vol. 11, no. 17, pp. 4115–4125, Nov. 2017.
- [26] T.-H. Chen, M.-S. Chen, T. Inoue, P. Kotas, and E. A. Chebli, "Three-phase cogenerator and transformer models for distribution system analysis," *IEEE Trans. Power Deliv.*, vol. 6, no. 4, pp. 1671–1681, Oct. 1991.
- [27] A. Garces, "A linear three-phase load flow for power distribution systems," *IEEE Trans. Power Syst.*, vol. 31, no. 1, pp. 827–828, Jan. 2016.
- [28] M. Barni, F. Buti, F. Bartolini, and V. Cappellini, "A quasi-Euclidean norm to speed up vector median filtering," *IEEE Trans. Image Process.*, vol. 9, no. 10, pp. 1704–1709, Oct. 2000.
- [29] C. Seol and K. Cheun, "A Low Complexity Euclidean Norm Approximation," *IEEE Trans. Signal Process.*, vol. 56, no. 4, pp. 1721–1726, Apr. 2008.
- [30] *IEEE Recommended Practice for Monitoring Electric Power Quality*, IEEE Std. 1159.3-2019, 2019.
- [31] S. Karagiannopoulos, P. Aristidou, and G. Hug, "A Centralised Control Method for Tackling Unbalances in Active Distribution Grids," in *2018 Power Systems Computation Conference (PSCC)*, Dublin, Ireland, 2018.
- [32] G. K. V. Raju and P. R. Bijwe, "Efficient reconfiguration of balanced and unbalanced distribution systems for loss minimisation," *IET Gener. Transm. Dis.*, vol. 2, no. 1, pp. 7–12, January 2008.
- [33] R. Fourer, D. Gay, and B. Kernighan, *AMPL: A Modeling Language for Mathematical Programming*, 2nd ed. North Scituate, MA, USA: Duxbury press, 2003.
- [34] I. I. CPLEX, "V12.1: User's manual for CPLEX," *International Business Machines Corporation*, vol. 46, no. 53, p. 157, 2009.
- [35] W. H. Kersting, "Radial distribution test feeders," *IEEE Trans. Power Syst.*, vol. 6, no. 3, pp. 975–985, Aug. 1991.



Juan S. Giraldo (S'19, M'20) received the B.Sc. degree in electrical engineering from the Universidad Tecnológica de Pereira, Pereira, Colombia, in 2012, and the M.Sc. and Ph.D. degrees in electrical engineering from the University of Campinas, Campinas, Brazil, in 2015 and 2019, respectively. From Oct. 2019 to May 2021 he was a Postdoctoral Fellow at the Department of Electrical Engineering, Eindhoven University of Technology, Eindhoven, The Netherlands. He is currently a Researcher with the Mathematics of Operations Research group at the University of Twente, Enschede, The Netherlands. His current research interests include the optimization, planning, and control of electrical power systems, electricity markets, and machine learning applications to power systems.



Pedro P. Vergara (M'19) was born in Barranquilla, Colombia in 1990. He received the B.Sc. degree (with honors) in electronic engineering from the Universidad Industrial de Santander, Bucaramanga, Colombia, in 2012, and the M.Sc. degree in electrical engineering from the University of Campinas, UNICAMP, Campinas, Brazil, in 2015. In 2019, he received his Ph.D. degree from the University of Southern Denmark, SDU, Denmark, funded by the Sao Paulo Research Foundation (FAPESP). In 2019, he joined Eindhoven University of Technology, TU/e, in The Netherlands as a Postdoctoral Researcher. In 2020, he was appointed as Assistant Professor at the Intelligent Electrical Power Grids (IEPG) group at Delft University of Technology, also in The Netherlands. His main research interests include the development of methodologies for control, planning, and operation of electrical distribution systems with high penetration of low-carbon energy resources (e.g. electrical vehicles, PV systems, electric heat pumps) using optimization and machine learning approaches. Dr. Vergara has received the Best Presentation Award at the Summer Optimization School in 2018 organized by the Technical University of Denmark (DTU) and the Best Paper Award at the 3rd IEEE International Conference on Smart Energy Systems and Technologies (SEST), in Turkey, in 2020.



Juan Camilo López (M'19) received the double B.Sc. degrees in electronic engineering and electrical engineering from the Universidad Nacional de Colombia (UNAL), Manizales, Colombia, in 2011 and 2012, respectively. He received his M.Sc. degree in electrical engineering from Sao Paulo State University (UNESP), in Ilha Solteira, Brazil, in 2015, and the Ph.D. degree in electrical engineering at the State University of Campinas (UNICAMP), in Campinas, Brazil, in 2019. He is currently pursuing his postdoctoral studies at the School of Electrical and

Computer Engineering (FEEC) at UNICAMP. His research interests include development of methodologies for the optimization, planning, monetization, and control of electrical power systems.



Phuong Hong Nguyen (M'06) received the Ph.D. degree from the Eindhoven University of Technology, Eindhoven, The Netherlands, in 2010. Before joining the Environmental Research and Innovation (ERIN) Department, Luxembourg Institute of Science and Technology (LIST), in 2019, as the Group Leader of the Sustainable Energy Systems (SES) group. He has been holding an Assistant Professor position with tenure with the Electrical Energy System (EES) Group, Eindhoven University of Technology (TU/e). He was a Visiting Researcher

with the Real-Time Power and Intelligent Systems (RTPIS) Laboratory, Clemson University, USA, in 2012 and 2013. He has committed his research effort to realize synergies of advanced monitoring and control functions for the distribution networks along with emerging digital technologies. This distinctive combination of competences allows him to develop a research pathway crossing over various domains of mathematical programming, stochastics, data mining, and communication networks. His research interests include data analytics with deep learning, real-time system awareness using (IoT) data integrity, as well as predictive and corrective grid control functions.



Nikolaos G. Paterakis (S'14, M'15) received the Dipl. Eng. degree in Electrical and Computer Engineering from the Aristotle University of Thessaloniki, Thessaloniki, Greece, in 2013, and the Ph.D. degree in Industrial Engineering and Management from the University of Beira Interior, Covilha, Portugal, in 2015. From October 2015 to March 2017, he was a Postdoctoral Fellow with the Department of Electrical Engineering, Eindhoven University of Technology, Eindhoven, The Netherlands, where he is currently Assistant Professor. His current research

interests include electricity markets, power system operations and applications of machine learning and optimization techniques. Dr. Paterakis is an Associate Editor of the IET Renewable Power Generation, an Editor of MDPI Applied Sciences, and a Review Editor of Frontiers in Energy Research (Smart Grids). He has also been serving as a reviewer of more than 30 journals, while he was recognized as an Outstanding Reviewer of IEEE Trans. Sustainable Energy (2016) and as one of the Best Reviewers of IEEE Trans. Smart Grid (2015, 2017).